

PAPER • OPEN ACCESS

“Small wave number and less of Reynolds number inflow analysis in peristaltic transportation of “Hyperbolic tangent fluid” in curved channels by employing the influence of radial magnetic force”

To cite this article: T Sh Alshareef 2019 *IOP Conf. Ser.: Mater. Sci. Eng.* **571** 012010

View the [article online](#) for updates and enhancements.



IOP | ebooks™

Bringing you innovative digital publishing with leading voices to create your essential collection of books in STEM research.

Start exploring the collection - download the first chapter of every title for free.

"Small wave number and less of Reynolds number inflow analysis in peristaltic transportation of "Hyperbolic tangent fluid" in curved channels by employing the influence of radial magnetic force"

T Sh Alshareef

"Collage of education for pure science (Ibn Al- Haitham), University of Baghdad, Iraq"

["Tamaraalshareef@yahoo.com"](mailto:Tamaraalshareef@yahoo.com)

Abstract: Through this article, we studied the peristaltic motion of "Hyperbolic Tangent" fluid in the geometry of curvature channel by using the analysis of large wavelength and less of Reynolds number. The matter has controlled mathematically by the partial differential equations of continuity, motion, heat transfer. In the study, we used the impact of radial magnetic force. The obtained coupled non-linear equations of above equations have solved by an approximation technical. Locked formula solutions of the stream function, axial velocity, heat function has evaluated. The influence of curvature is analysed and took it into account. The impact of sundry variables on the inflow features have plotted and explained by graphs and figures.

Keyword: Hyperbolic tangent fluid, curved channel.

1. Introduction

The peristaltic motions at less of Reynolds number and prolonged wavelength have acquired more interest through the last years. The attention in these inflows is in order to their many applications either in engineering or medical process. Such these applications implicate the pee transportation from urinary tract, gall from the gall bladder into the duodenum, spermatozoa in the ductus efferent of the male reproductive tract, ovum in the fallopian tube, lymph in the lymphatic vessel et Cetera.

Historical brief of the peristalsis transportation is come back to T. W. [1]. In 1969, A. H. et al. [2] examined increase of wavelength and less of Reynolds number approaches. Various investigators in this area have posteriorly pressed these studies.

It has noted from the standing studies that more of the papers that have published on the peristaltic motion include the flux geometries of planar channels or tubes. To the better of our knowing, H. Sato et al. [3] have been the first author who tested the two-dimensional peristaltic motion of a viscous fluid in a curvature channel. This considered geometry of the channel has possible implementations in physiology since more of the glandular ducts have curved; also, this type of channels has industrial applications. See [4, 5]



Various efforts have taken by thinking physiological fluids as Newtonian. A small number of discussions with respect to peristaltic motion of Newtonian fluids have presented in [6 -8] Further, some motivating studies has advanced in life fluid physiographic fluids such as blood which can charities' by the models of (power-law, casson and Herschel- Bulkley), chime (Williamson model), loaf and white eggs through esophagus (Maxwell model) and urine contagion (couple-stress model) to be non-Newtonian through pumping for details , see [9-11]. Among these non- Newtonian fluids, the model of the hyperbolic tangent describe the inflow manner of shear thinning fluids (that is the viscosity of fluid will be decrease with an increasing of shear stress). Nadeem et al [12] addressed the peristaltic pumping of a hyperbolic tangent fluid through an asymmetric channel, for more details see [13].

Peristaltic motion with heat transfer impacts has be hard done by number of researches in order to attitude different suggestion in bio-medical and biomechanical sciences. The biological of temperature transfer in a living system contain thermal conduction in tissue, metabolic heat generation, burn injuries, haven, exudation of blood inflow) and hyperthermia. See [14-16] .

The effect of magnetic force possibly helpful to ease up the blood flux in human arterial system, central the blood inflow velocities in surgical operations.

Recently, Nadeem et al [17] presented mathematical model to the peristaltic transportation of hyperbolic tangent fluid by helping the properties of curvature of the symmetric channel. Abbas, et al. [18] studied the three dimensional of peristaltic motion of hyperbolic tangent fluid by using the features of flexible walls.

So, there is no attempt to study the peristaltic transport of hyperbolic tangent fluid in curved geometrical channel by using the effects of magnetic force and heat /mass transfer. Therefore we use the influence of radial magnetic field in our work, besides the effect of heat and mass transfer by studding the impact of Brinkmann number (Br), The equations of the system have reduced subject to lubrication approach and then have solved by using an approximation method of perturbation analysis. Function formulation for the stream function, velocity, temperature have adopted. The results of the problem have discussed graphically.

2. Mathematical Pattern

Let us consider a channel of thickness (2a) coiled in a circle with center (o) and radius (R). An incompressible fluid of hyperbolic tangent fluid (H-T) fill out the channel. The axial and radial directions have denoted by \bar{X} and \bar{r} respectively. Inflow in the channel has happened come back to expansion of peristaltic waves moving on the channel walls in the axial direction with constant speed C. The geometry of peristaltic walls has given by the following relation: (see fig. (1)).

$$\bar{H}(\bar{x}, \bar{t}) = \bar{r}a \mp b \cos\left[\frac{2\pi}{\lambda}(\bar{x} - c\bar{t})\right] \quad \dots(1)$$

Where $+\bar{H}(\bar{x}, \bar{t})$ is the upper wall, $-\bar{H}(\bar{x}, \bar{t})$ is the lower wall, (b) is the wave amplitude, λ is the wavelength and \bar{t} is the time. Velocity field for such motion is $v = [\bar{v}(\bar{r}, \bar{x}, \bar{t}), \bar{u}(\bar{r}, \bar{x}, \bar{t}), \bar{t}]$

With respect to curvilinear coordinates (\bar{r}, \bar{x}) .

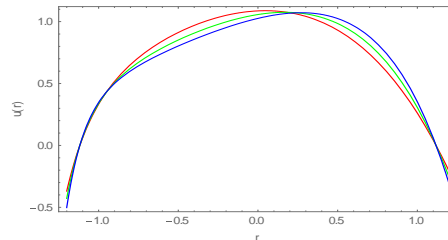


Figure 1: The relation of peristaltic walls

In this problem, the fluid is electrically conducting and is following under the influence of radially varying magnetic field of the form [19]:

$$\bar{B} = \frac{RB_0}{R+r} e_r \tag{2}$$

This type of magnetic field satisfies the Maxwell equations. The Lorentz force \bar{F} in view of the magnetic can given by:

$$\bar{F} = \bar{J} \times \bar{B} = [0, -\sigma(\frac{R}{R+r})^2 B_0^2 \bar{U}, 0] \tag{3}$$

Where B_0 is the strength of applied magnetic field, σ is the electric conductivity of fluid, \bar{J} is the current density.

3. Constitutive Equations

The equations that have been controlled the shear stress of hyperbolic tangent fluid has given by: [13]

$$\bar{\tau} = [\mu_\infty + (\mu_0 + \mu_\infty) \tanh(\Gamma \dot{\bar{y}})^n] \dot{\bar{y}} \tag{4}$$

$$\dot{\bar{y}} = \sqrt{\frac{1}{2} \sum_i \sum_j \dot{\bar{y}}_{ij} \dot{\bar{y}}_{ji}} = \sqrt{\frac{1}{2} \Pi}, \quad \Pi = \text{trace } D^2 \text{ and } D^2 = \text{grad} \bar{v} + (\text{grad} \bar{v})^t \text{ for } \mu_\infty = 0$$

and $(\Gamma \dot{\bar{y}}) < 1$, equation(4) can written as:

$$\bar{t} = [\mu_0 \tanh(\Gamma \dot{\bar{y}})^n] \dot{\bar{y}} = \mu_0 [1 + (\Gamma \dot{\bar{y}} - 1)]^n = \mu_0 [1 + n(\Gamma \dot{\bar{y}} - 1)] \dot{\bar{y}} \tag{5}$$

Here μ_0 is the zero shear-rate viscosity, low index of hyperbolic tangent fluid and $\text{grad} \bar{v}$ denotes the gradient of the velocity vector.

The stress components \bar{t}_{rr} , \bar{t}_{xr} and \bar{t}_{xx} can obtained through the following relations:

$$\bar{t}_{rr} = \mu_0 [1 + n(\Gamma \dot{\bar{y}} - 1)] \bar{y} \cdot 2 \frac{\partial \bar{V}}{\partial r} \tag{6}$$

$$\bar{t}_{xr} = \mu_0 [1 + n(\Gamma \dot{\bar{y}} - 1)] \left(\frac{\partial \bar{U}}{\partial r} + \frac{R}{r+R} \frac{\partial \bar{V}}{\partial X} - \frac{\bar{U}}{r+R} \right) \tag{7}$$

$$\bar{t}_{xx} = \mu_0 [1 + n(\Gamma \dot{\bar{y}} - 1)] \cdot 2 \left(\frac{R}{r+R} \frac{\partial \bar{U}}{\partial X} + \frac{\bar{V}}{r+R} \right) \tag{8}$$

Where $\dot{\bar{y}}$ is the shear rate and dots over the quantities indicate differentiation with respect to time.

$$\dot{\bar{y}} = \sqrt{2 \left(\frac{\partial \bar{V}}{\partial r} \right)^2 + \left(\frac{\partial \bar{U}}{\partial r} + \frac{R}{r+R} \frac{\partial \bar{V}}{\partial X} - \frac{\bar{U}}{r+R} \right)^2 + 2 \left(\frac{R}{r+R} \frac{\partial \bar{U}}{\partial X} + \frac{\bar{V}}{r+R} \right)^2} \tag{9}$$

4. Basic Governing Equations

The main equations that governing the non-Newtonian incompressible viscous named here by hyperbolic tangent fluid have given by the equations of (continuity, momentum and energy equations that described by temperature and concentration equations) as follows:

$$\frac{R}{r+R} \frac{\partial \bar{U}}{\partial X} + \frac{\partial \bar{V}}{\partial r} + \frac{\bar{V}}{r+R} = 0 \tag{10}$$

$$\rho \left(\frac{\partial \bar{V}}{\partial t} + \bar{V} \frac{\partial \bar{V}}{\partial r} + \frac{R}{r+R} \bar{U} \frac{\partial \bar{V}}{\partial X} - \frac{\bar{U}^2}{r+R} \right) = - \frac{\partial \bar{P}}{\partial r} + \frac{1}{r+R} \frac{\partial}{\partial r} \{ (r+R) \bar{t}_{rr} \} + \frac{R}{r+R} \frac{\partial}{\partial X} \bar{t}_{xr} - \frac{1}{r+R} \bar{t}_{xx} \tag{11}$$

$$\rho \left(\frac{\partial \bar{U}}{\partial t} + \bar{V} \frac{\partial \bar{U}}{\partial r} + \frac{R}{r+R} \bar{U} \frac{\partial \bar{U}}{\partial X} - \frac{\bar{U} \bar{V}}{r+R} \right) = - \frac{R}{r+R} \frac{\partial \bar{P}}{\partial X} + \frac{R}{(r+R)} \frac{\partial}{\partial X} \bar{t}_{xx} + \frac{1}{(r+R)^2} \frac{\partial}{\partial r} \{ (r+R)^2 \bar{t}_{xr} \} - \sigma \left(\frac{R}{r+R} \right)^2 B_0^2 \bar{U} \tag{12}$$

The temperature equation has given by:

$$\rho C_p \left(\frac{\partial}{\partial t} + \bar{V} \frac{\partial}{\partial r} + R \frac{\bar{U}}{r+R} \frac{\partial}{\partial X} \right) T = k_1 \left[\frac{\partial^2 T}{\partial r^2} + \frac{1}{r+R} \frac{\partial T}{\partial r} + \left(\frac{R}{r+R} \right)^2 \frac{\partial^2 T}{\partial X^2} \right] + (\bar{t}_{rr} - \bar{t}_{xx}) \left[\frac{\partial \bar{U}}{\partial r} + \frac{R}{r+R} \frac{\partial \bar{V}}{\partial X} - \frac{\bar{U}}{r+R} \right] \tag{13}$$

Where \bar{P} is the pressure, ρ is the density, C_p is the specific heat, k_1 is the thermal conductivity, (T) is the fluid temperature.

5. Methodology of the Problem

With a view to simplify the system of governing and constitutive equations of the problem, we can introduce the following dimensionless transformations as follows:

$$\begin{aligned}
 x &= \frac{\bar{X}}{\lambda}, r = \frac{\bar{r}}{a}, t = \frac{c\bar{t}}{\lambda}, u = \frac{\bar{U}}{c}, v = \frac{\bar{V}}{\sigma c}, h = \frac{\bar{H}}{a}, p = \frac{a^2 \bar{P}}{\mu_0 c \lambda}, \sigma = \frac{a}{\lambda}, k = \frac{R}{a}, \theta = \frac{T - T_0}{T_0}, \\
 \phi &= \frac{b}{a}, \text{Re} = \frac{\rho c a}{\mu_0}, M^2 = \frac{\sigma B_0^2 a^2}{\mu_0}, k^2 = \frac{d^2}{k_0}, \text{Pr} = \frac{\mu_0 C \rho}{k_1}, \text{Ec} = \frac{c^2}{C \rho (T_0)}, t_{rr} = \frac{\lambda}{\mu_0 c} \bar{t}_{rr}, t_{xr} = \\
 \frac{a}{\mu_0 c} \bar{t}_{xr}, t_{xx} &= \frac{a}{\mu_0 c} \bar{t}_{xx}, y = \frac{a}{c} \bar{y}, \text{We} = \frac{\Gamma c}{a}, \text{Br} = \text{Pr Ec}, u = -\frac{\partial \psi}{\partial r}, v = \frac{k}{r+k} \frac{\partial \psi}{\partial x} \dots(14)
 \end{aligned}$$

Where (Re) is the Reynolds number, (F) is the volume flow rate, σ is the wave number, ϕ is the amplitude ratio, (k) is the curvature parameter, (Pr) is the prandtl number, (Ec) is the Eckert number, (ψ) is the stream function, (Br) is Brinkman number, (θ) is the temperature distribution, (M) is Hartmann number, (we) is the wiessenberg number, Γ is the time constant, (T_0) is the temperature of the fluid at the upper and lower parts of the channel, (u) is the axial velocity, (v) is the radial velocity. Using the above dimensionless quantities, the equations (10-13) become as follows:

$$\frac{k}{r+k} \frac{\partial u}{\partial x} + \frac{\partial v}{\partial r} + \frac{v}{r+k} = 0 \tag{15}$$

$$\begin{aligned}
 \text{Re} \sigma \left(\sigma^2 \frac{\partial v}{\partial t} + \sigma^2 v \frac{\partial v}{\partial r} + \sigma^2 \frac{k}{r+k} u \frac{\partial v}{\partial x} - \frac{u^2}{r+k} \right) &= -\frac{\partial p}{\partial r} + \frac{\sigma^2}{r+k} \frac{\partial}{\partial r} \{ (r+k) t_{rr} \} + \frac{\sigma^2 k}{r+k} \frac{\partial}{\partial x} t_{xr} \\
 -\frac{1}{r+k} \sigma t_{xx} & \dots(16)
 \end{aligned}$$

$$\begin{aligned}
 \text{Re} \sigma \left(\frac{\partial u}{\partial t} + v \frac{\partial u}{\partial r} + \frac{k}{r+k} u \frac{\partial u}{\partial x} - \frac{uv}{r+k} \right) &= -\frac{k}{r+k} \frac{\partial p}{\partial x} + \frac{k}{r+k} \sigma \frac{\partial}{\partial x} t_{xx} + \frac{1}{(r+k)^2} \frac{\partial p}{\partial r} \\
 \{ (r+k)^2 t_{xr} \} - \left(\frac{k}{r+k} \right)^2 M^2 u & \dots(17)
 \end{aligned}$$

$$\begin{aligned}
 \text{Re Pr} \sigma \left(\frac{\partial \theta}{\partial t} + v \frac{\partial \theta}{\partial r} + \frac{k}{r+k} u \frac{\partial \theta}{\partial x} \right) &= \frac{\partial^2 \theta}{\partial r^2} + \frac{1}{r+k} \frac{\partial \theta}{\partial r} + \left(\frac{k}{r+k} \right)^2 \sigma^2 \frac{\partial^2 \theta}{\partial x^2} + \text{Br} \sigma (\sigma t_{rr} - t_{xx}) \\
 \frac{\partial v}{\partial r} + \text{Br} t_{xx} \left(\frac{\partial u}{\partial r} + \sigma^2 \frac{k}{r+k} \frac{\partial v}{\partial x} - \frac{u}{r+k} \right) & \dots(18)
 \end{aligned}$$

With non-dimensional variables, the stress components are:

$$t_{rr} = 2[1 + n(\text{we} \dot{y} - 1)] \frac{\partial v}{\partial r} \tag{20}$$

$$t_{xr} = [1 + n(\text{we} \dot{y} - 1)] \left(\frac{\partial u}{\partial r} + \frac{k}{r+k} \sigma^2 \frac{\partial v}{\partial x} - \frac{u}{r+k} \right) \tag{21}$$

$$t_{xx} = 2\sigma [1 + n(\text{we} \dot{y} - 1)] \left(\frac{k}{r+k} \frac{\partial u}{\partial x} + \frac{v}{r+k} \right) \tag{22}$$

$$\dot{y} = \sqrt{2\sigma^2 \left[\left(\frac{\partial v}{\partial r} \right)^2 + \left(\frac{k}{r+k} \frac{\partial u}{\partial x} + \frac{v}{r+k} \right)^2 \right] + \left(\frac{\partial u}{\partial r} + \frac{k}{r+k} \sigma^2 \frac{\partial v}{\partial x} - \frac{u}{r+k} \right)^2} \tag{23}$$

The general solution of the governing equations (16-23) in the general case appears to be difficult, so we can reduce the analysis under the assumption of small wavelength ($\sigma \ll 1$) and low Reynolds number approach, thus we can rewrite the previous equations under these approximations as follows:

$$\frac{\partial p}{\partial x} = \frac{1}{k(r+k)} \frac{\partial}{\partial r} \{(r+k)^2 t_{xr}\} - \left(\frac{k}{r+k}\right) M^2 u \quad \dots(24)$$

$$\frac{\partial p}{\partial r} = 0 \quad \dots(25)$$

$$0 = \frac{\partial^2 \theta}{\partial r^2} + \frac{1}{r+k} \frac{\partial \theta}{\partial r} + Br t_{rx} \left(\frac{\partial u}{\partial r} - \frac{u}{r+k} \right) \quad \dots(26)$$

$$t_{rr} = 2[1 + n(we \dot{y} - 1)] \frac{\partial v}{\partial r} \quad \dots(27)$$

$$t_{xr} = [1 + n(we \dot{y} - 1)] \left(\frac{\partial u}{\partial r} - \frac{u}{r+k} \right) \quad \dots(28)$$

$$t_{xx} = 0 \quad \dots(29)$$

$$\dot{y} = \frac{\partial u}{\partial r} - \frac{u}{r+k} \quad \dots(30)$$

The corresponding dimensionless boundary conditions have given by:

$$\psi = \mp \frac{F}{2}, \text{ at } r = \pm h = \pm(1 + \phi \cos 2\pi(x-t))$$

$$\frac{\partial \psi}{\partial r} = 0, \text{ at } r = \mp h, \theta = 0 \text{ at } r = \mp h \quad \dots(31)$$

The relation between volume flow rate and time average flow rate is: [20]

$$F(x,t) = Q + 2h(x,t) - 1 \quad \dots(32)$$

6. Perturbed System and Perturbation Solutions

The equations (24), (26) are not linear and their exact solutions are not easy to obtain. Therefore, we used the perturbation approximation technique with small values of weissenberg number in the form of:

$$\psi = \psi_0 + We \psi_1 + o(we^{(2)})$$

$$u = u_0 + We u_1 + o(we^{(2)})$$

$$\theta = \theta_0 + We \theta_1 + o(we^{(2)})$$

$$p = p_0 + We p_1 + o(we^{(2)}) \dots$$

$$F = F_0 + We F_1 + o(we^{(2)}) \quad \dots(33)$$

6.1 Perturbed Systems

6.1.1 Zeroth-Order System

$$\frac{\partial p_0}{\partial x} = \frac{1-n}{k} [-(r+k) \cdot \left(\frac{\partial^3 \psi_0}{\partial r^3} \right) - \left(\frac{\partial^2 \psi_0}{\partial r^2} \right) + \frac{1}{r+k} \frac{\partial \psi_0}{\partial r}] + \frac{k}{r+k} M^2 \frac{\partial \psi_0}{\partial r} \quad \dots(34)$$

$$0 = \frac{1-n}{k} ((r+k) \cdot \frac{\partial^4 \psi_0}{\partial r^4} + 2 \frac{\partial^3 \psi_0}{\partial r^3} - \frac{1}{(r+k)} \frac{\partial^2 \psi_0}{\partial r^2} + \frac{1}{(r+k)^2} \frac{\partial \psi_0}{\partial r} - k^2 M^2 (\frac{1}{(r+k)} \cdot \frac{\partial^2 \psi_0}{\partial r^2} - \frac{1}{(r+k)^2} \frac{\partial \psi_0}{\partial r})) \dots(35)$$

$$0 = \frac{\partial^2 \theta_0}{\partial r^2} + \frac{1}{(r+k)} \frac{\partial \theta_0}{\partial r} + Br(1-n) \{ (\frac{\partial^2 \psi_0}{\partial r^2})^2 - \frac{2}{(r+k)} \cdot \frac{\partial^2 \psi_0}{\partial r^2} \cdot \frac{\partial \psi_0}{\partial r} + \frac{1}{(r+k)^2} (\frac{\partial \psi_0}{\partial r})^2 \} \dots(36)$$

Along the corresponding boundary conditions:

$$\begin{aligned} \psi_0 &= \frac{-F_0}{2}, \frac{\partial \psi_0}{\partial r} = 0, \theta_0 = 0, \text{ at } (r = +h) \\ \psi_0 &= \frac{F_0}{2}, \frac{\partial \psi_0}{\partial r} = 0, \theta_0 = 0, \text{ at } (r = -h) \end{aligned} \dots(37)$$

6.1.2 First-Order System

$$\begin{aligned} \frac{\partial p_1}{\partial x} &= -\frac{(1-n)}{k} (r+k) \frac{\partial^3 \psi_1}{\partial r^3} - \frac{(1-n)}{k} \frac{\partial^2 \psi_1}{\partial r^2} + \frac{1-n}{k(r+k)} \frac{\partial \psi_1}{\partial r} + \frac{2n}{k} (r+k) \frac{\partial^2 \psi_0}{\partial r^2} \frac{\partial^3 \psi_0}{\partial r^3} \\ &- \frac{2n}{k} \frac{\partial \psi_0}{\partial r} \frac{\partial^3 \psi_0}{\partial r^3} + \frac{k}{r+k} \cdot M^2 \frac{\partial \psi_1}{\partial r} \end{aligned} \dots(38)$$

$$0 = -\frac{(1-n)}{k} (r+k) \frac{\partial^4 \psi_1}{\partial r^4} + 2 \frac{(1-n)}{k} \frac{\partial^3 \psi_1}{\partial r^3} - \frac{(1-n)}{k} (\frac{1}{r+k} \frac{\partial^2 \psi_1}{\partial r^2} - \frac{1}{(r+k)^2} \frac{\partial \psi_1}{\partial r}) - \frac{2n}{k} (r+k) (\frac{\partial^2 \psi_0}{\partial r^2} \frac{\partial^4 \psi_0}{\partial r^4} + (\frac{\partial^3 \psi_0}{\partial r^3})^2) + \frac{2n}{k} \frac{\partial \psi_0}{\partial r} \frac{\partial^4 \psi_0}{\partial r^4} - k \cdot M^2 [\frac{1}{r+k} \frac{\partial^2 \psi_1}{\partial r^2} - \frac{1}{(r+k)^2} \frac{\partial \psi_1}{\partial r}] \dots(39)$$

$$\begin{aligned} 0 &= \frac{\partial^2 \theta_1}{\partial r^2} + \frac{1}{(r+k)} \frac{\partial \theta_1}{\partial r} + Br(1-n) \{ 2 \frac{\partial^2 \psi_0}{\partial r^2} \frac{\partial^2 \psi_1}{\partial r^2} - \frac{2}{(r+k)} \cdot (\frac{\partial^2 \psi_0}{\partial r^2} \cdot \frac{\partial \psi_1}{\partial r} + \frac{\partial^2 \psi_1}{\partial r^2} \cdot \frac{\partial \psi_0}{\partial r}) \\ &+ \frac{2}{(r+k)^2} \cdot \frac{\partial \psi_0}{\partial r} \frac{\partial \psi_1}{\partial r} + Bm \{ -(\frac{\partial^2 \psi_0}{\partial r^2})^3 + \frac{3}{r+k} (\frac{\partial^2 \psi_0}{\partial r^2})^2 \frac{\partial \psi_0}{\partial r} - \frac{3}{r+k} (\frac{\partial \psi_0}{\partial r})^2 \frac{\partial^2 \psi_0}{\partial r^2} + \\ &\frac{1}{(r+k)^3} (\frac{\partial \psi_0}{\partial r})^3 \} \end{aligned} \dots(40)$$

With the corresponding boundary conditions:

$$\begin{aligned} \psi_1 &= \frac{-F_1}{2}, \frac{\partial \psi_1}{\partial r} = 0, \theta_1 = 0, \text{ at } (r = +h) \\ \psi_1 &= \frac{F_1}{2}, \frac{\partial \psi_1}{\partial r} = 0, \theta_1 = 0, \text{ at } (r = -h) \end{aligned} \dots(41)$$

6.2 Perturbation Solutions

6.2.1 Zeroth-order Solution

If we solve the equations (35)-(36), we have the following solutions

$$\begin{aligned} \psi_0 &= a_4 + a_3kr + \frac{a_3r^2}{2} + a_2n_3(k+r)^{1-n_1} + a_1n_2(k+r)^{1+n_1}; \\ \theta_0 &= \frac{a_2^2Br(-1+n)(-1+n1^2)^2n_3^2(k+r)^{-2n_1}}{4n1^2} + \frac{a_1^2Br(-1+n)(-1+n_1^2)^2n_2^2(k+r)^{2n_1}}{4n1^2} \\ &+ c_2 + c_1Log[k+r] + a_1a_2Br(-1+n)(-1+n1^2)^2n_2n_3Log[k+r]^2; \end{aligned}$$

Where a_i, c_j ($i = 1, 2, 3, 4, j = 1, 2$) constants can obtained by using boundary conditions (37) and working on "Mathematica Program"

6.2.2 First order solution

Substituting the Zeroth-order solutions of (42)-(45) into equations (38)-(41) and then solving the resulting system with the corresponding boundary conditions, we get:

$$\begin{aligned} \psi_1 &= b_4 + b_3kr + \frac{b_3r^2}{2} + b_2n_3(k+r)^{1-n_1} - a_2^2nn_3^2n_4(k+r)^{-2n_1} - a_1^2nn_2^2n_5(k+r)^{2n_1} \\ &+ b_1n_2(k+r)^{1+n_1}; \\ \theta_1 &= c_4 + \frac{1}{12}(6a_3Bm(a_3^2k(-3+2k) - 12a_1a_2(-1+n_1^2)n_2n_3)r + 3a_3^3Br(-3+4k)nr^2 \\ &+ 4a_3^3Bmr^3 + \frac{1}{(1-3n_1)^2n_1}4a_1^3Bm(1+n_1)n_2^3(k+r)^{-1+3n_1}(-3n_2^5 + 3n_1^6 + k(-1+2n_1 \\ &+ 3n_1^2)^2 - 3n_1^4(5+8(-1+n)n_5 - 3r) + r + 12n_1^3(-1+4(-1+n)n_5+r) - \dots \end{aligned}$$

Where b_i, c_j ($i = 1, 2, 3, 4, j = 1, 2, 3, 4$) constants can obtained by using boundary conditions (37) and working on "Mathematica Program"

7. Analysis and Discussion

In this section, the numerical and computation results have discussed for the problem. (Mathematica) software is used to find out the graphs of more intersect parameters.

7.1 Velocity profile

Velocity equations is function of radial coordinate impact of various variables on the velocity distribution have shown in figures (2-8). From figure (2-a) the effect of parameter M on u has displayed, it is noticed that at the region (-1, 0) the velocity will be less than the magnitude of velocity at the region (0, 1). The effects of variables on ϕ & Q on axial velocity u are explained in figure (3-a) and (4-a) respectively, we observed that the velocity will be rise up at both parts of channel with an increase of these variables opposite manner for the influence of axial coordinate x and is sketched in fig.(5-a). The performance of parameters (n) and (we) is displayed in figures (6-a) and (7), it is noticed that the velocity will be increase at the upper wall of channel and the case will be conversely at the lower part of the channel. The attitude of curvature coordinates is noted in figure (8), it is realized that the velocity will decrease at the upper wall and will increase at the lower part of the channel with an increase of small values of (k). the effectiveness of symmetry of the channel will be appear by clear coordinates as we observed in figures(2-b)-(6-b) respectively.

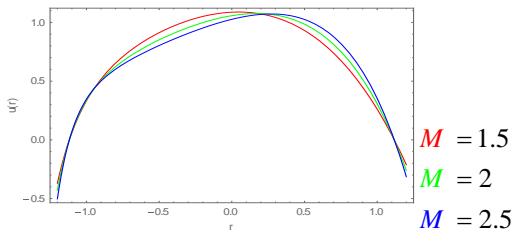


Figure (2-a). Effect of (M) on velocity u
 $\phi = 0.2, t = 0.05, n = 0.5, we = 0.01,$
 $Q = 1.5, x = 0.2$ when ($k = 2$)

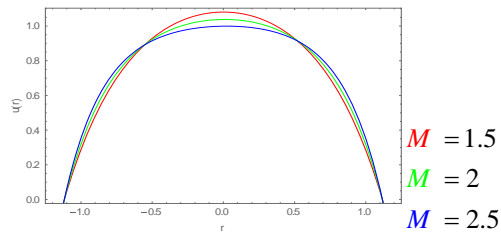


Figure (2-b). Effect of (M) on velocity u
 $\phi = 0.2, t = 0.05, n = 0.5, we = 0.01,$
 $Q = 1.5, x = 0.2$ when ($k = 50$)

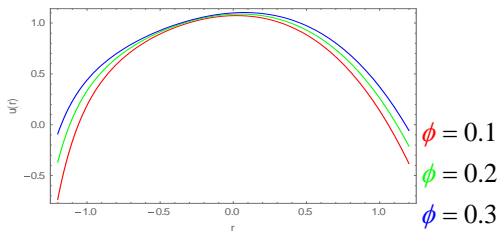


Figure (3-a). Effect of (ϕ) on velocity u
 $M = 1.5, t = 0.05, n = 0.5, we = 0.01,$
 $Q = 1.5, x = 0.2$ when ($k = 2$)

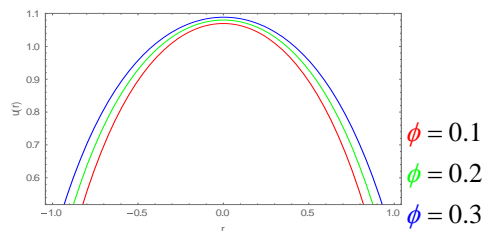


Figure (3-b). Effect of (ϕ) on velocity u
 $M = 1.5, t = 0.05, n = 0.5, we = 0.01,$
 $Q = 1.5, x = 0.2$ when ($k = 50$)

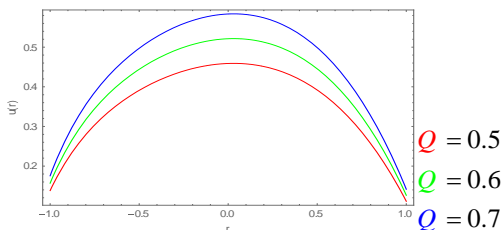


Figure (4-a). Effect of (Q) on velocity u
 $M = 1.5, t = 0.05, n = 0.5, we = 0.01,$
 $\phi = 0.2, x = 0.2$ when ($k = 2.5$)

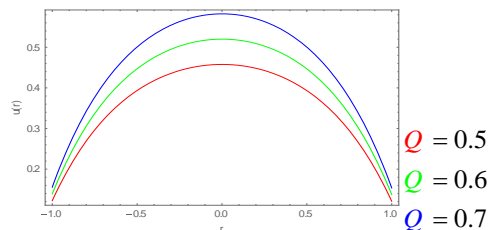


Figure (4-b). Effect of (Q) on velocity u
 $M = 1.5, t = 0.05, n = 0.5, we = 0.01,$
 $\phi = 0.2, x = 0.2$ when ($k = 50$)

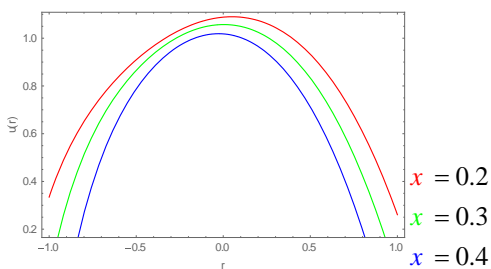


Figure (5-a). Effect of (x) on velocity u
 $M = 1.5, t = 0.05, n = 0.5, we = 0.01,$
 $\phi = 0.2, Q = 1.5$ when ($k = 1.9$)

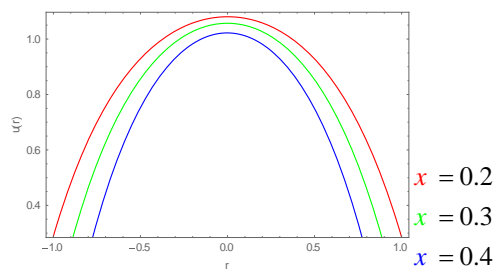


Figure (5-b). Effect of (x) on velocity u
 $M = 1.5, t = 0.05, n = 0.5, we = 0.01,$
 $\phi = 0.2, Q = 1.5$ when ($k = 50$)

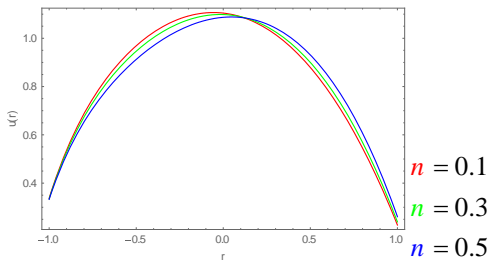


Figure (6-a). Effect of (n) on velocity u
 $M = 1.5, t = 0.05, \phi = 0.2, we = 0.01,$
 $Q = 1.5, x = 0.2$ when ($k = 2$)

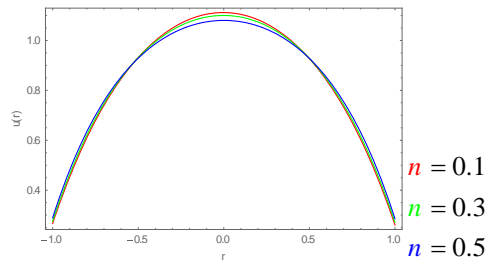


Figure (6-b). Effect of (n) on velocity u
 $M = 1.5, t = 0.05, \phi = 0.2, we = 0.01,$
 $Q = 1.5, x = 0.2$ when ($k = 50$)

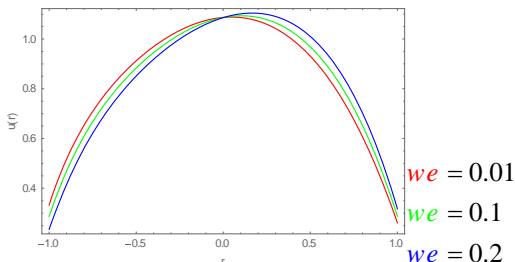


Figure (7). Effect of (we) on velocity u
 $M = 1.5, t = 0.05, \phi = 0.2, n = 0.5$
 $Q = 1.5, x = 0.2$ when ($k = 2$)

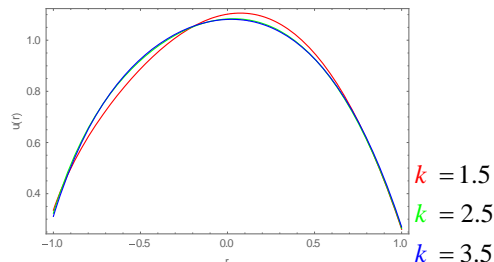


Figure (8). Effect of (k) on velocity u
 $M = 1.5, t = 0.05, \phi = 0.2, n = 0.5$
 $Q = 1.5, x = 0.2, we = 0.01$

7.2 Temperature profile
 Temperature's equations are function of (r). Temperature distributions have been sketched in figures (9-15)

to study the influences of the variables M, Br, n, k, we and Q with fixed values of $x = (0.2)$ and $t = (0.05)$. Figure (9-a) and (10) are drawn to study the effect of M and k on temperature distributions θ , we see that the temperature decrease with an increase of above parameters. Similar behavior for the influence of n on temperature and it is shown in figure (11-a). Figures (12-a) and (13-a) display the effect of Br and ϕ , we noted that the temperature will be excess with an increase of these variables. Similarly the effect of Q on temperature profile and it is seen in figure (14-a). It has observed that graphs of temperature is symmetric with a large value of curvature coordinates (k) as we noticed in the figures (9-b)-(14-b).

In figure (15-a) the impact of (we) on temperature have given, we noticed that the magnitude of temperature will be small with small values of (k) and at large values of k , the temperature will be clearly small in the upper wall and it starts to increase in the lower part of channel as shown in figure (15-b).

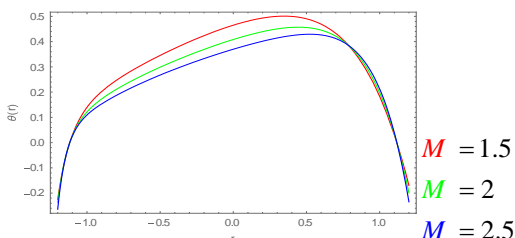


Figure (9-a). Effect of (M) on temperature
 $\phi = 0.2, t = 0.05, Br = 2, n = 0.5, we = 0.01,$
 $Q = 1.5, x = 0.2$ when ($k = 2$)

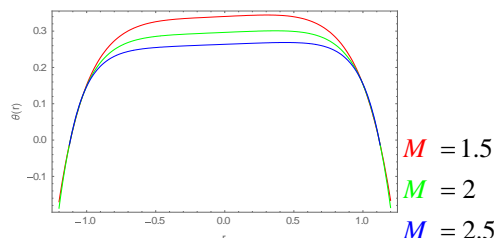


Figure (9-b). Effect of (M) on temperature
 $\phi = 0.2, t = 0.05, Br = 2, n = 0.5, we = 0.01,$
 $Q = 1.5, x = 0.2$ when ($k = 20$)

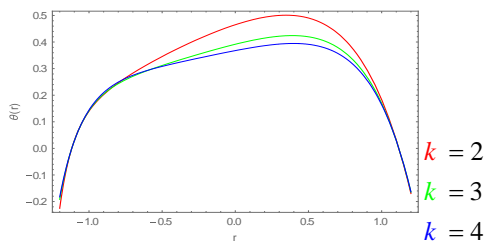


Figure (10-a). Effect of (k) on temperature $\phi = 0.2, t = 0.05, Br = 2, n = 0.5, we = 0.01, Q = 1.5, x = 0.2, M = 1.5$

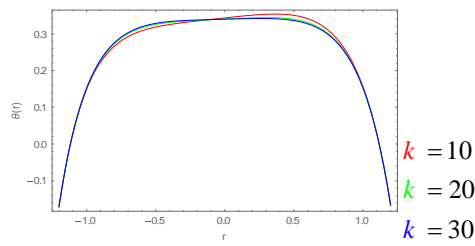


Figure (10-b). Effect of (k) on temperature $\phi = 0.2, t = 0.05, Br = 2, n = 0.5, we = 0.01, Q = 1.5, x = 0.2, M = 1.5$

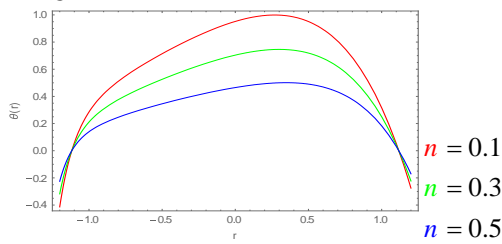


Figure (11-a). Effect of (n) on temperature $\phi = 0.2, t = 0.05, Br = 2, we = 0.01, Q = 1.5, x = 0.2, M = 1.5, \text{ when } (k = 2)$

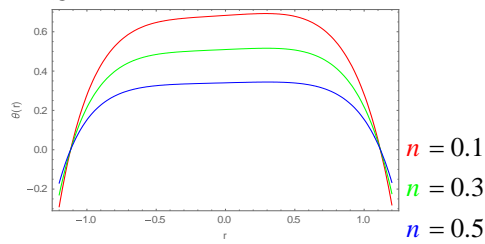


Figure (11-b). Effect of (n) on temperature $\phi = 0.2, t = 0.05, Br = 2, we = 0.01, Q = 1.5, x = 0.2, M = 1.5, \text{ when } (k = 20)$

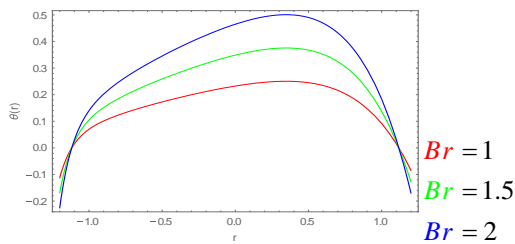


Figure (12-a). Effect of (Br) on temperature $\phi = 0.2, t = 0.05, we = 0.01, n = 0.5, Q = 1.5, x = 0.2, M = 1.5, \text{ when } (k = 2)$

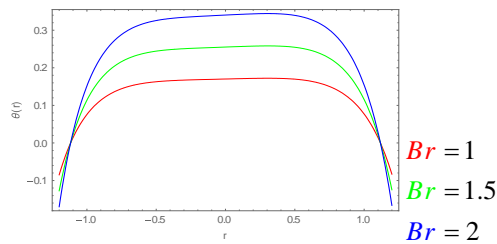


Figure (12-b). Effect of (Br) on temperature $\phi = 0.2, t = 0.05, we = 0.01, n = 0.5, Q = 1.5, x = 0.2, M = 1.5, \text{ when } (k = 20)$

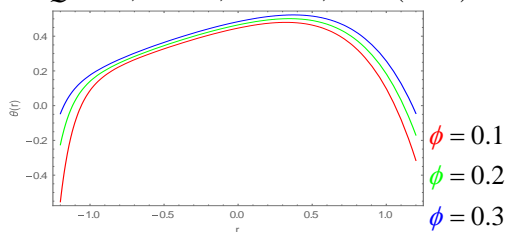


Figure (13-a). Effect of (ϕ) on temperature $t = 0.05, we = 0.01, n = 0.5, Br = 2, Q = 1.5, x = 0.2, M = 1.5, \text{ when } (k = 2)$

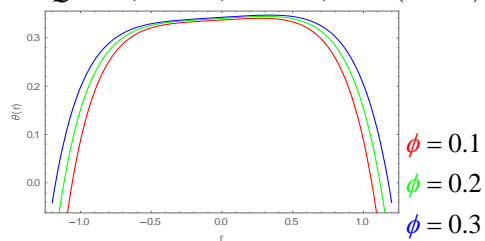


Figure (13-b). Effect of (ϕ) on temperature $t = 0.05, we = 0.01, n = 0.5, Br = 2, Q = 1.5, x = 0.2, M = 1.5, \text{ when } (k = 2)$

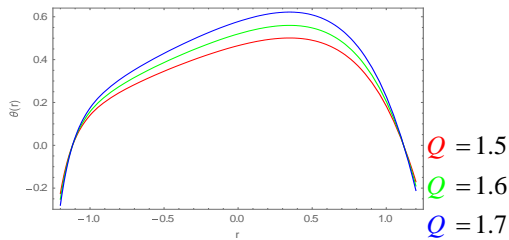


Figure (14-a). Effect of (Q) on temperature $\phi = 0.2, t = 0.05, we = 0.01, n = 0.5$
 $Br = 2, x = 0.2, M = 1.5$, when ($k = 2$)

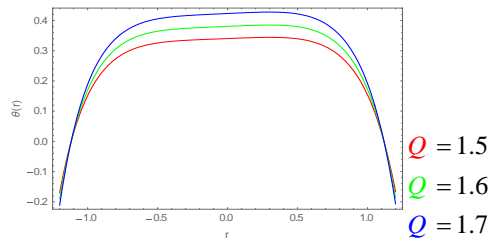


Figure (14-b). Effect of (Q) on temperature $\phi = 0.2, t = 0.05, we = 0.01, n = 0.5$
 $Br = 2, x = 0.2, M = 1.5$, when ($k = 20$)

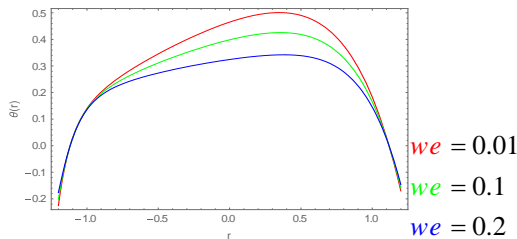


Figure (15-a). Effect of (we) on temperature $\phi = 0.2, t = 0.05, Q = 1.5, n = 0.5$
 $Br = 2, x = 0.2, M = 1.5$, when ($k = 2$)

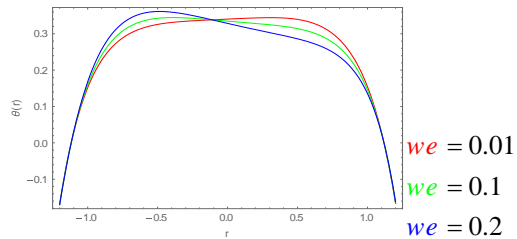
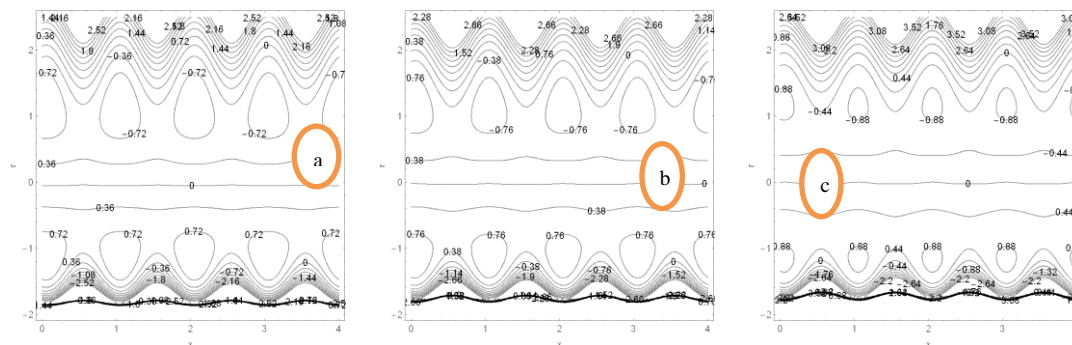


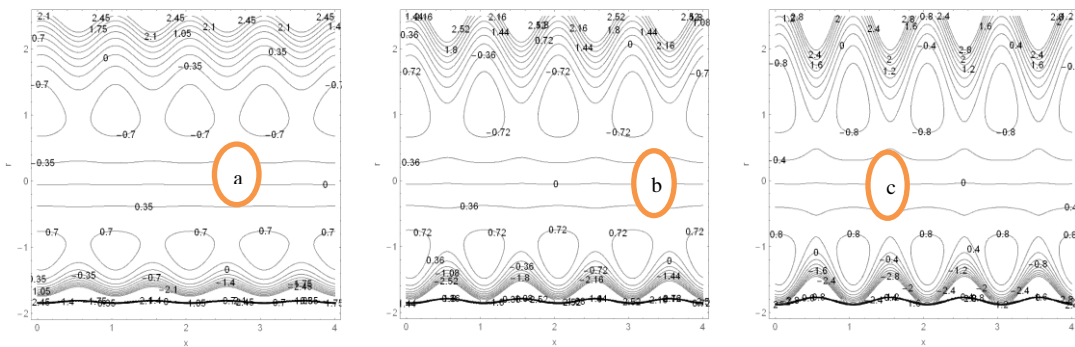
Figure (15-b). Effect of (we) on temperature $\phi = 0.2, t = 0.05, Q = 1.5, n = 0.5$
 $Br = 2, x = 0.2, M = 1.5$, when ($k = 20$)

7.3 Phenomenon of Trapping

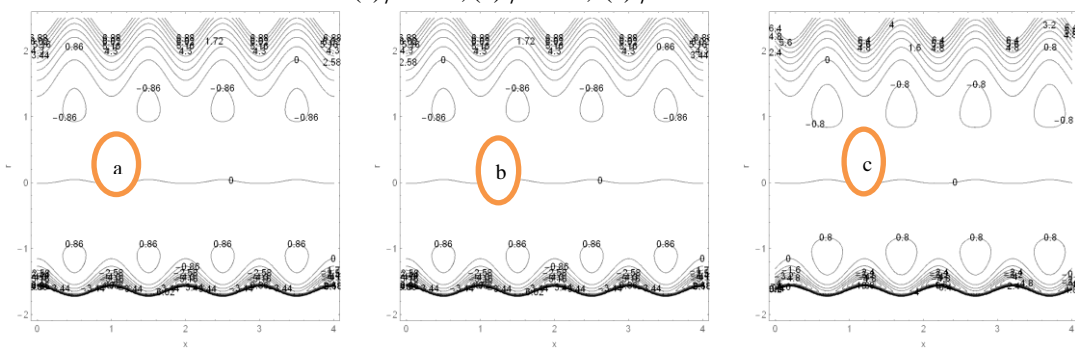
The influence of sundry variables like M, ϕ, t, n, we, k and Q on trapping can show over figures (16-22). Figure (16), display that the size of trapped bolus decrease with an increase of M in the two parts of channel. Figure (17) has plotted for the impact of (ϕ) on trapping. It can be seen that the bolus will be change have taken elongation in their appearance with an increase of ϕ . Similarly action for the effect of (t) on trapping bolus and is shown in figure (18). Figures (19) and (20) are plotted for the behavior of n and we and it is observed rameters, we not that the bolus have been less in the two walls of channel, viscous and Newtonian fluid ($we=0, n=0$) is greater than the bolus in the Hyperbolic tangent fluid ($we \neq 0, n \neq 0$). The effect of k on trapping is noticed in figure (21), it is noted that the bolus is appeared to be shrinkable with high values of k . figure (22), have offered the influence of Q , it is seen that the bolus are disparate in size in the both sides of walls at the small values of Q , with an increase of that parameter, we remarked that the bolus will be less in number and size. In the all above effects of parameters, we noticed that bolus would be symmetric at the both parts of channel.



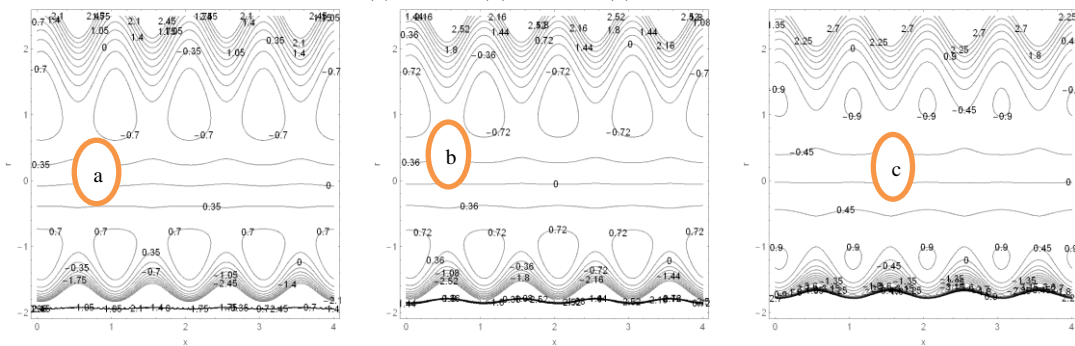
Figure(16): effect of (M) on stream line for (a) $M = 1$, (b) $M = 1.3$, (c) $M = 1.5$



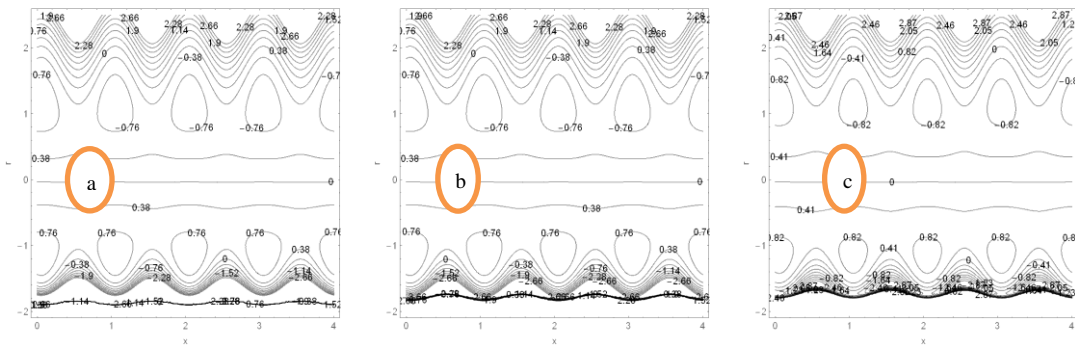
Figure(17): effect of (ϕ) on stream line for (a) $\phi = 0.1$, (b) $\phi = 0.2$, (c) $\phi = 0.3$



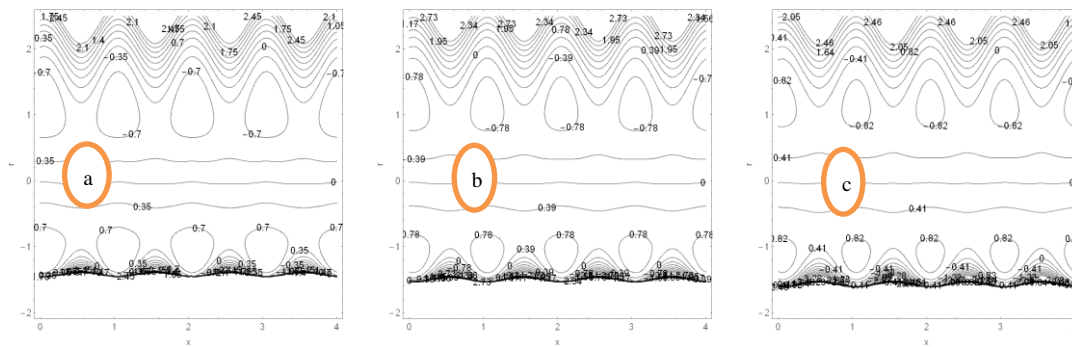
Figure(18): effect of (t) on stream line for (a) $t = 0.5$, (b) $t = 1.5$, (c) $t = 1.7$



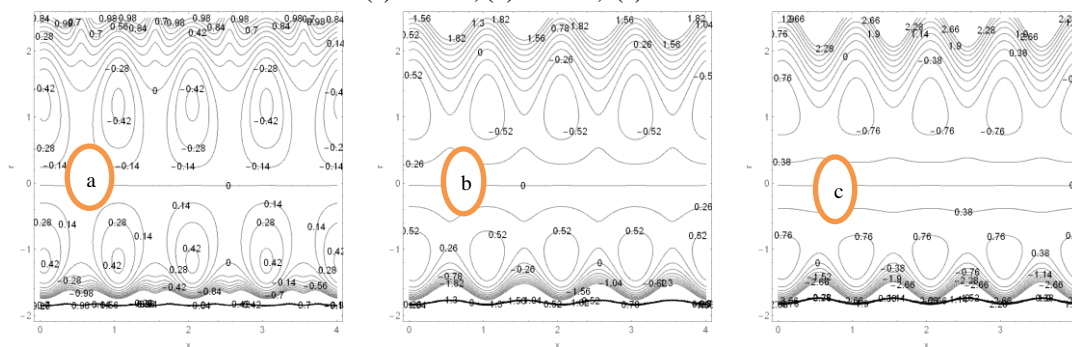
Figure(19): effect of (n) on stream line for (a) $n = 0.1$, (b) $n = 0.5$, (c) $n = 0.7$



Figure(20): effect of (we) on stream line for (a) $we = 0.0001$, (b) $we = 0.001$, (c) $we = 0.003$



Figure(21): effect of (k) on stream line for (a) $k = 1.5$, (b) $k = 1.6$, (c) $k = 1.7$



Figure(22): effect of (Q) on stream line for (a) $Q = 0.5$, (b) $Q = 1$, (c) $Q = 1.5$

Figures (16-22) Effects of parameters on stream line for $\phi = 0.2, t = 0.05, M = 1, we = 0.001, n = 0.5, k = 2, Q = 1.5$

8. Produced Notes

This problem deals with the common impacts of radial magnetic force and heat transfer on the peristaltic transport of incompressible hyperbolic tangent in curvature channel. We got the approximate solutions of the problem under the assumptions of large wavelength and less of Reynolds number and the results of non-linear coupled equations are be solved by using perturbation analysis. The numerical commutations were analyzed for different values of variables namely Hartmann number (M), amplitude ratio ϕ , curvature parameter k, time flow rate Q, parameters of hyperbolic tangent fluid (we and n) and Brinkman number (Br). So through our work we noticed the following observations:

1. The velocity of the fluid has increased with an increase of ϕ and Q in all regions of channel, reverse case is satisfied for an increase of x.
2. The velocity of the using fluid will be increased at the upper part of the channel and decreased at the lower part of channel with an increase of M, (we) and (n). Conversely, situation has observed for an increase of k.
3. The graph of velocity distribution will be more symmetrical with more increasing values of curvature variable k at most of parameters.
4. The graph of velocity distribution will be wanes at the center of the channel with an increase of (M), (we) and (n) at more high values of (k).

5. The temperature of the fluid is an increasing function of ϕ, Br and Q . Opposite case is an increasing of M, n, k and we .
6. The temperature of fluid which is used in this problem is observed to be low in comparison with viscous fluid ($we=0, n=0$)
7. The graphic of temperature distribution is noted to be symmetric at most of variables with more rising values of k .
8. The size of the trapping bolus will be increased with an increase of ϕ, t , adverse status is obtained for an increase of M, n, k and we .
9. The shape of the bolus is seen to be symmetric at both sides of channel with an increasing of M, ϕ, t, n, we and k .
10. The bolus is observed to be dissimilar at small values of Q in the both walls of channel, and these bolus is started to be more small in size and numbered with more increasing values of Q .
11. If we put $M=0$, in our problem we obtained a study paper of S. Nadeem and E. N. Maraj. [17].

References

- [1] Latham, T. W., 1966, *Fluid Motion in Peristaltic Pump*, M. S. Thesis, MIT Cambridge MA.
- [2] Shapiro, A. H., Jaffrin, M. Y. and Weinberg, S. L., 1969, Peristaltic Pumping With Long Wave Lengths at Low Reynolds Number, *J. Fluid Mech.* 37, 799.
- [3] Sato, H., Kawai, T., Fujita, T. and Okabe, M., 2000 *Trans. Japan Soc. Mech. Eng B*, 66,679.
- [4] Hayat, T. Naseema Aslam, Rafiq, M. and Alsaedi, A., 2017, studying peristaltic transport of shape nano size silver water nano materials in digestive system with heat generation, *Int. J. Heat and Mass transfer*, 106, 18-24.
- [5] Hayat, T., Maryiam, J. and Awatif Hendi, A., 2011, Peristaltic transport of viscous fluid in a curved channel with compliant walls, *Int. J. Heat and Mass transfer*, 54, 1615-1621.
- [6] Jaffrin, M. Y. and Shapiro, A. H., 1971, Peristaltic Pumping, *Annual Rev. fluid Mech.* (3), 13-37.
- [7] Miltra, T. K. and Prasad, S. N., 1973, on the influence of wall properties and poiseuille flow in peristalsis, *Journal of Biomechanics*, (6), 681-693.
- [8] Shukla, J. B., Parihar, R. S., Rao, B. R. P., Gupta, S. P., 1980, Effects of peripheral-layer viscosity on peristaltic transport of a bio-fluid, *Journal of Mechanics*, (97)(2), 225-237.
- [9] Raju, K. K. and Devanathan, R., 1972, Peristaltic motion of non-Newtonian fluid, *Rheological Acta*, (11)(2), 170-178.
- [10] Vajravelu, K., Sreenadh, S. and Ramesh Babu, V., 2005, Peristaltic transport of altershel-Bulkley fluid in an inclined tube, *Int. J. non-linear Mech.* (40), 83-90.
- [11] Pandey, Sk. and Tripathi, D., 2010, influence of magnetic field on the peristaltic flow of viscous fluid through finite-length cylindrical tube, *Applied Bionics and Biomechanics*, (7) (3), 169-176.
- [12] Nadeem, S. and Akram, S., 2009, Peristaltic transport of a hyperbolic tangent fluid model in an asymmetric channel, *Zietschrift Fur Natur for Schung A.* (64), 559-567.
- [13] Saravana, R., Hemadri Reddy, R., Swresh goud, J. and Sreenadh, S., 2017, MHD Peristaltic flow of a hyperbolic tangent fluid in a non-uniform channel with heat and mass transfer, *IOP Conf. Series: Materials Science and Engineering*, (263).
- [14] Akbar, N. S. and Nadeem, S., 2012, Peristaltic flow of phan-thien-Tanner nono fluid in adiverging tube, *Heat transfer Res*, (41), 10-22.

- [15] Akbar, N. S. and Nadeem, S., 2010, Simulation of heat and chemical reactions on Reiner Rivlin model for blood flow through a tapered artery with stenosis, *Int. J. Heat and mass transfer*, (46), 531-539.
- [16] Hayat, T. and Hina, S., 2010, the influences of wall properties on the MHD peristaltic flow of a Maxwell fluid with heat and mass transfer, *nonlinear Anal. Real world Appl.* (4)(4), 3155-3169.
- [17] Nadeem, S. and Maraj, E. N., 2013, the Mathematical Analysis for peristaltic flow of Hyperbolic Tangent fluid in a curved channel, *communications in theoretical physics*, (59) (6).
- [18] Ali Abbas, M., Bai, Y. Q. and Rashidi, M. M., 2016, three dimensional peristaltic flow of hyperbolic tangent fluid in non-uniform channel having flexible walls, *Alexendria Engineering Journal*, (55), 653-662.
- [19] Hayat, T., Zahir, H., Tanveer, A., Alsaedi, A., Soret and Dufour, Effects on MHD peristaltic transport of Jeffrey fluid in curved channel with convective boundary conditions, *plos one*, (2(2)), E0164854, *Journal pone*.
- [20] Narla, V. K., Prasad, K. M. and Raman ammurthy, J. V., 2015, Peristaltic transport of Jeffrey nano fluid in curved channels, *Procedia Engineering*, (127), 869-876.